

## Magnesium Chloride increases apoptosis and decreases prostate cancer cells migration

Julianna Maria Santos<sup>1</sup>, Fazle Hussain<sup>2\*</sup>

<sup>1</sup>Texas Tech University, Mechanical Engineering Department (TTU), <sup>2</sup>Internal Medicine, and Cell Physiology and Molecular Biophysics (TTUHSC), Lubbock, Texas, USA

**Corresponding Author:** Fazle Hussain, Texas Tech University, Mechanical Engineering Department (TTU), Internal Medicine, and Cell Physiology and Molecular Biophysics (TTUHSC), Lubbock, Texas, USA

**Submission Date:** June 10th, 2017, **Acceptance Date:** January 27th, 2017, **Publication Date:** January 31st, 2017

**Citation:** Santos J.M., Hussain F., Magnesium Chloride increases apoptosis and decreases prostate cancer cells migration. *Functional Foods in Health and Disease* 2018; 8(1): 62-78. DOI: <https://doi.org/10.31989/ffhd.v8i1.368>

### ABSTRACT

**Background:** Reduced levels of magnesium can cause several diseases and increase cancer risk. Motivated by magnesium chloride's (MgCl<sub>2</sub>) non-toxicity, physiological importance, and beneficial clinical applications. This study aims to study its action mechanism and possible mechanical, molecular, and physiological effects in prostate cancer with different metastatic potentials.

**Methods:** We examined the effects of MgCl<sub>2</sub>, after 24 and 48 hours, on apoptosis, cell migration, expression of epithelial mesenchymal transition (EMT) markers, and V-H<sup>+</sup>-ATPase, myosin II (NMII) and the transcription factor NF Kappa B (NFkB) expressions.

**Results:** MgCl<sub>2</sub> induces apoptosis, and significantly decreases migration speed in cancer cells with different metastatic potentials. MgCl<sub>2</sub> reduces the expression of V-H<sup>+</sup>-ATPase and myosin II that facilitates invasion and metastasis, suppresses the expression of vimentin and increases expression of E-cadherin, suggesting a role of MgCl<sub>2</sub> in reversing the EMT. MgCl<sub>2</sub> also significantly increases the chromatin condensation and decreases NFkB expression.

**Conclusions:** These results suggest a promising preventive and therapeutic role of MgCl<sub>2</sub> for prostate cancer. Further studies should explore extending MgCl<sub>2</sub> therapy to in vivo studies and other cancer types.

**Keywords:** Magnesium chloride, prostate cancer, migration speed, V-H<sup>+</sup>-ATPase, EMT

## BACKGROUND

Magnesium ( $Mg^{2+}$ ) is the fourth most common cation in the human body, and it has a crucial role as a co-factor in more than 300 enzymatic reactions related to energy metabolism and nucleic acid synthesis [1, 2].  $Mg^{2+}$  is also involved in several physiological processes such as hormone receptor binding, gating of calcium channels, transmembrane ion flux, muscle contraction, neuronal activity, vasomotor tone control, cardiac excitability, and neurotransmitter release. Diet and lifestyles significantly impact the risk factors associated with prostate cancer [2] and can greatly arrest cancer progression [3]. Studies have shown the benefits of  $Mg^{2+}$  supplementation for several medical conditions such as eclampsia, preeclampsia, arrhythmia, severe asthma, and migraine. Furthermore, there are beneficial results such as improved glucose and insulin metabolism, alleviated dysmenorrhea, and leg cramps in women [1, 4]. Chronic low levels of  $Mg^{2+}$  are associated with several severe diseases, including diabetes, hypertension, coronary heart disease, and osteoporosis [1, 5].  $Mg^{2+}$  homeostasis is usually maintained by renal regulation of  $Mg^{2+}$  reabsorption, although the exact mechanism of this regulation is not understood [1]. Cisplatin treatment has the side effect of inducing  $Mg^{2+}$  deficiency that enhances nephrotoxicity [6]. As a result,  $Mg^{2+}$  supplementation improves the adverse effects of cisplatin and decreases renal toxicity in cancer patients treated with cisplatin (by causing significant changes in plasma creatinine and urea levels) [7]. Epidemiologic studies have shown that  $Mg^{2+}$  intake may decrease the risk of colorectal cancer (CRC), although this observation is not universal [8].

Cancer cells are known to over-regulate many proteins (such as V- $H^+$ -ATPase) that enhance their metastatic potentials and facilitate invasion of neighboring tissues and launch metastasis. V- $H^+$ -ATPase on the cancer cell plasma membrane acidifies the extracellular environment by extruding protons which activates metalloproteinases that digest the extracellular matrix to promote invasion and metastasis [9, 10]. Because of epithelial mesenchymal transition (EMT), the marker vimentin is over-regulated while F-actin and E-Cadherin are down-regulated. EMT, a reversible process that causes changes in cell shape, behavior, and motility, may facilitate cancer metastasis [11–15]. EMT usually occurs in embryo formation, wound healing, and malignant transformation [16].

Prostate adenocarcinoma is the most common male cancer in the United States, with 1 in every 4 newly diagnosed cancers belonging to this category [17]. The cause and progression of prostate cancer are not well understood; the poor prognosis of prostate carcinoma is widely recognized [18]. We used prostate cancer as an experimental model due to its high incidence and lethality [17]. The therapeutic effect of  $MgCl_2$  in cancer cells is underexplored, with the action mechanism remaining unknown. So far, only one recent study demonstrated increased apoptosis induced by treatment with  $MgCl_2$  in one specific prostate cancer cell line [2].

We discovered  $MgCl_2$  can be an effective preventive therapeutic agent for prostate cancer because of its effect in decreasing cell growth and migration via down-regulating V- $H^+$ -ATPase, in addition to reversing the EMT process via decreasing vimentin expression and increasing F-actin and E-Cadherin. Furthermore,  $MgCl_2$  shows beneficial effects in several diseases besides cancer. Further studies are required to understand the action mechanism of  $MgCl_2$  and establish the relevant metabolic pathways.

## METHODS

### *Cell Lines and Culture*

All cells were cultured at 37°C in a 5% CO<sub>2</sub> environment. Prostate cancer cells (LNCaP, DU145, CL2, and PC3) were provided by Dr. Stephanie Filleur (Texas Tech University Health Sciences Center, Lubbock, TX). Cells were cultured in RPMI 1640 medium with L-glutamine (Gibco, 10-040-CV, Thermo Fisher Scientific, Massachusetts, USA), supplemented with 5% fetal bovine serum (FBS) (Gibco, 10437-028, Thermo Fisher Scientific, Massachusetts, USA). LNCaP cells had an additional supplement of 1% penicillin-streptomycin antibiotics (Gibco, 15140-122). For every passage, cells were harvested using trypsin for 2 minutes (Gibco by Life Technologies, 25302-062 - 5ml per flask) at 37°C for DU145, CL2, and PC3, and 1 minute for LNCaP. Trypsin was inhibited by adding 500 µl FBS, and then cells were placed in a conic tube and centrifuged for 5 minutes at 1000 rpm (Eppendorf Centrifuge 5804R, Hauppauge, New York, USA). The supernatant was removed, and cells were suspended in 2-4 ml fresh medium and counted with trypan blue (Corning, 25900CI, New York, USA) using an automated cell counter (TC20, Bio-Rad, Berkeley, California, USA). LNCaP cells are lowly metastatic and have androgen receptors and low rates of growth [19]. DU145, a moderately metastatic cell line that does not express androgen receptors, was obtained from a brain metastasis [20]. CL2 is a LNCaP parental, has a highly metastatic phenotype, and is androgen receptor insensitive [19, 21]. PC3 is a highly metastatic cell line that does not express androgen receptors [21] and was obtained from a bone metastasis [22].

### *Cell Viability Assay*

Cells were plated in a 12 well plate until sub-confluent and then treated with 500 µM MgCl<sub>2</sub> in culture medium (Sigma-Aldrich, M4880) for 48 hours. Control cells were grown in culture medium. After 48 hours, the medium was removed from the wells and 100 µl annexin V binding buffer was added (422201, BioLegend, California, USA) along with the stain annexin V alexa fluor 488 (Invitrogen by Life Technologies, A13201, Carlsbad, California, USA, 5 µl in 100 µl buffer). Cells were incubated for 15 minutes at room temperature. Next, the stain was removed and 100 µl annexin V binding buffer was added. Images were acquired with a Nikon Eclipse motorized microscope (Nikon Instruments Inc., New York, USA) using GFP filter (488nm). Magnification 20x.

### *Monolayer Wound Scratch Assay*

Cells were seeded in a 12 well plate. After total confluence, a wound was made in each well using a 10 µl pipette tip [23]. The medium was removed, cells rinsed with DPBS (Corning, 21-031-CV) to remove debris, and a fresh medium containing 5% FBS was added. MgCl<sub>2</sub> was added to culture medium at concentrations of 25 µM, 50 µM, 200 µM, 500 µM, and 1 mM. The wound scratch assay was imaged every 10 minutes for 24 hours using a Nikon Eclipse motorized microscope with an incubator at 5% CO<sub>2</sub> and 37°C. The migration speed was calculated by subtracting the initial from the final wound widths and dividing by the elapsed time.

### ***Subcellular Fractionation***

Prostate cells were trypsinized, washed twice with cold PBS, and resuspended in 3 ml of homogenizer buffer containing 1.3 M sucrose (Sigma-Aldrich S7903i, St. Louis, Missouri, USA), 1 mM MgCl<sub>2</sub> (Sigma-Aldrich, M4880), and 10 mM potassium phosphate buffer pH 6.8 (Sigma-Aldrich, P5379) supplemented with a protease inhibitor cocktail (Thermo Fisher Scientific, 88265) at a concentration of one tablet per 50 ml. Cells were homogenized 20 times in a Teflon /glass dounce homogenizer. The suspension was then stored as a homogenate fraction (containing all cellular fractions including plasma membrane, cytosol, and nucleus) at -80°C. The protein concentration was determined with a spectrophotometer/fluorometer (DeNovix, DS-11 FX+, Wilmington, Delaware, USA) using the nano drop function at 280 nm prior to performing western blots.

### ***Fluorescence Staining***

Cells were plated on coverslips until sub-confluence reached and then treated with 500 μM MgCl<sub>2</sub> for 48 hours. Control cells were maintained in just the cell culture medium. After 48 hours, cells were fixed with 4% paraformaldehyde, quenched with Phosphate Buffer Saline (PBS) with 50 mM NH<sub>4</sub>Cl (Sigma-Aldrich, 213330) for 10 minutes, permeabilized with 0.1% PBS-Triton for 10 minutes, blocked with 1% PBS-BSA (Sigma-Aldrich, A2153) for 15 minutes, and incubated for 1 hour with alexa fluor phalloidin 488 (dilution 1:300 in PBS-BSA, Molecular probes by Life Technologies A12379, Eugene, Oregon) that specifically stains F-actin (filaments). After staining, the coverslips were washed 7 times with PBS and mounted on glass slides using Prolong Gold antifade reagent with the nuclear stain DAPI (Molecular probes by Life Technologies, P36935). Images were obtained at 90x using a Nikon Eclipse motorized microscope.

### ***Western Blots***

Homogenate fractions (30μg protein), the control, and samples treated with MgCl<sub>2</sub> (500 μM), were diluted 1:1 in laemmli sample buffer (Bio-Rad,161-0737) with 50 μl 2-mercaptoethanol (Bio-Rad,161-0710), placed in 4-20% gradient acrylamide gels (Bio-Rad,456-8093), and separated by electrophoresis. Samples from the gels were transferred to nitrocellulose membranes (Bio-Rad,170-4158) using the Trans-Blot system (Bio-Rad, 170-4155). Membranes were incubated for 1 hour in a 3% milk, Phosphate Buffer Saline (PBS), and Tween solution on a plate shaker (blocked). The blocking solution was made from 3 g of milk powder (Nestle, nonfat dry milk, Glendale, California, USA), dissolved in 100 ml of PBS with Tween. PBS was prepared by mixing (for each liter) KCl 2.7 mM (Sigma-Aldrich, P3911), KH<sub>2</sub>PO<sub>4</sub> 1.47 mM (Sigma-Aldrich, P5379), Na<sub>2</sub>HPO<sub>4</sub> 8.1 mM (Sigma-Aldrich, S9763), and NaCl 137 mM (Fisher Chemical, S641-212). Tween was added to PBS (Bio-Rad,170-6531, 1:1000 dilution) at the time of the experiment. Then membranes were incubated with primary antibodies for V-H<sup>+</sup>-ATPase c subunit (Developmental Studies Hybridoma Bank, 224-256-2-s,dilution 1:100), myosin II (NMIIB) (Developmental Studies Hybridoma Bank, CMII23, dilution 1:500), vimentin (Developmental Studies Hybridoma Bank, AMF-17b-s, dilution 1:300), E-Cadherin (Cell Signaling, #14472, Beverly, Massachusetts - dilution 1:1000), and transcription factor NFκB (Developmental Studies Hybridoma Bank, PRCP-NFκB1-2B9, dilution 1:300) for 2

hours at 37°C.  $\beta$ -actin was used as loading control (Sigma-Aldrich, A3854 -dilution 1:25000). Membranes were washed 2 times in the PBS-Tween solution for 5 minutes. Finally, the membranes were incubated with horseradish peroxidase-conjugated secondary antibodies anti-mouse IgG (JacksonImmuno Research,115035068, West Grove, Pennsylvania) and anti-rabbit IgG (JacksonImmuno Research,111036003, dilution for secondary antibodies 1:1000) for 1 hour at 37°C. The blots were revealed using ECL solution (Bio-Rad,170-5060) and visualized using an image analyzer system (Bio-Rad,ChemiDocMP, 1708265). Expression levels were quantified using ImageJ software. All blots were normalized from the loading  $\beta$ -actin control.

## RESULTS

### *MgCl<sub>2</sub> Induces Apoptosis*

To address if MgCl<sub>2</sub> (500  $\mu$ M) treatment induces apoptosis, we performed an assay that specifically stains apoptotic cells [24]. Fluorescent images of apoptotic cells stained by annexin V (Fig. 1, A-H) shows that 48 hours of MgCl<sub>2</sub> treatment significantly increased the number of apoptotic cells. This data confirms that apoptosis occurred in prostate cancer cells both with (LNCaP) and without (DU145, CL2, and PC3) androgen receptors.

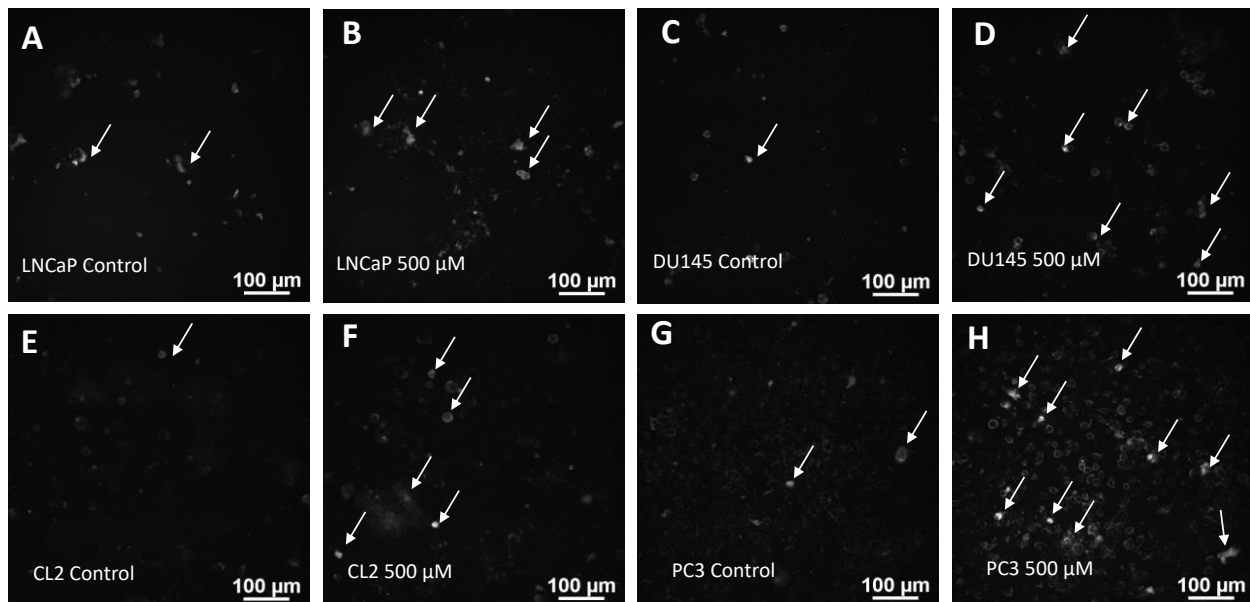


**Figure 1.** MgCl<sub>2</sub> induces apoptosis in prostate cancer cells. Prostate cancer cells LNCaP (A and B), DU145 (C and D), CL2 (E and F), and PC3 (G and H) control and after 48 hours of MgCl<sub>2</sub> treatment (500  $\mu$ M) showing annexin V positive cells (arrows). Pictures acquired using Nikon Eclipse, GFP filter; n=3.

### *MgCl<sub>2</sub> Significantly Decreases the Cell Migration Speed*

We studied the impact of MgCl<sub>2</sub> on cell migration. Prostate cancer cell migration was evaluated by a monolayer wound scratch assay in control condition and after MgCl<sub>2</sub> (24 hours, 25  $\mu$ M, 50  $\mu$ M, 200  $\mu$ M, 500  $\mu$ M, and 1mM). The most effective concentration for all cells was 500  $\mu$ M (Fig. 2) that decreased the migration speed of LNCaP by 34 % (Fig. 2A), DU145 by 29% (Fig. 2B), CL2 by 23% (Fig. 2C), and PC3 (Fig. 2D) by 35%, compared to control. These results demonstrate that MgCl<sub>2</sub> impairs cell motility. Additionally, even at

low concentrations  $MgCl_2$  significantly reduced the migration speed of the highly metastatic cells (PC3) by 26%, 29%, 21%, 35%, and 32% at concentrations of 25, 50, 200, 500  $\mu M$ , and 1 mM respectively (Fig. 2D).

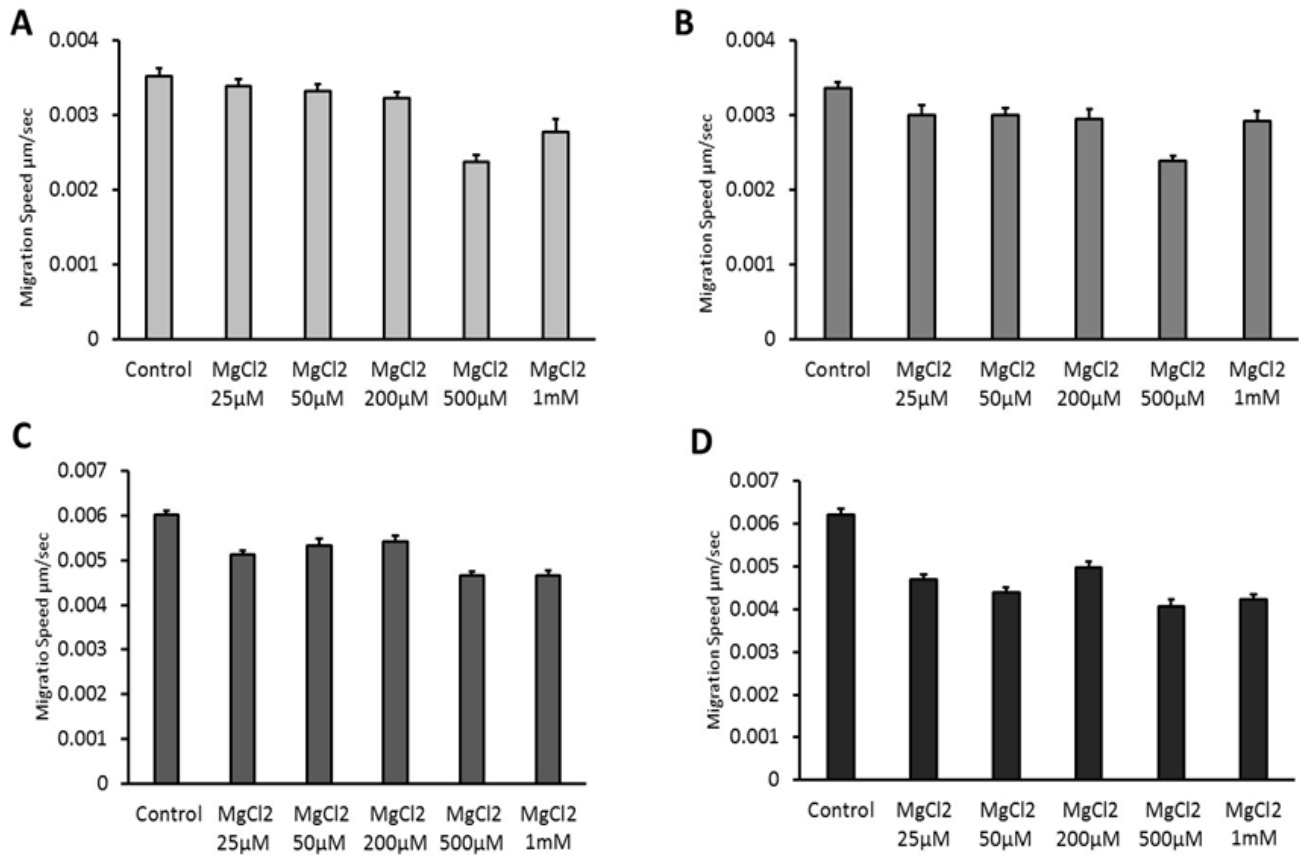


**Figure 2.**  $MgCl_2$  decreases significantly the migration speed in prostate cancer cells. LNCaP (A), DU145 (B), CL2 (C) and PC3 (D) control and after 24 hours of  $MgCl_2$  treatment at specific concentrations: 25  $\mu M$ , 50  $\mu M$ , 200  $\mu M$ , 500  $\mu M$ , and 1mM. The speed was calculated from wound scratch assay pictures by subtracting the final wound gap from the initial (time 0); n=4. One way ANOVA tests: (A) LNCaP: control vs. 500  $\mu M$  ( $p < 0.001$ ) and 1mM ( $p < 0.001$ ); (B) DU145: control vs. 25  $\mu M$  ( $p = 0.010$ ), 50  $\mu M$  ( $p = 0.017$ ), 200  $\mu M$  ( $p = 0.005$ ), 500  $\mu M$  ( $p < 0.001$ ), and 1mM ( $p = 0.022$ ); (C) CL2: control vs. 25  $\mu M$ , 200  $\mu M$ , 500  $\mu M$ , and 1mM ( $p < 0.001$ ), 50  $\mu M$  ( $p = 0.009$ ); (D) PC3: control vs. 25  $\mu M$ , 50  $\mu M$ , 200  $\mu M$ , 500  $\mu M$ , and 1mM;  $p < 0.001$  all cases.

### ***MgCl<sub>2</sub> Decreases the Expression of V-H<sup>+</sup>-ATPase***

Highly metastatic tumors have at the plasma membrane a high expression and activity of V-H<sup>+</sup>-ATPase (proton pump) that act as the main regulator of membrane potential. This pump acidifies the extracellular environment that activates proteases to promote invasion and metastasis [25]. Due to this key function of proton pumps in cancer cells, we addressed whether  $MgCl_2$  is able to decrease V-H<sup>+</sup>-ATPase expression in prostate cancer cells. Figure 3 shows the expression and quantification of V-H<sup>+</sup>-ATPase subunit c in LNCaP (Fig. 3A), DU145 (Fig. 3B), CL2 (Fig. 3C), and PC3 (Fig. 3D).  $MgCl_2$  decreases the expression of V-H<sup>+</sup>-ATPase by more than 30% in all prostate cells.

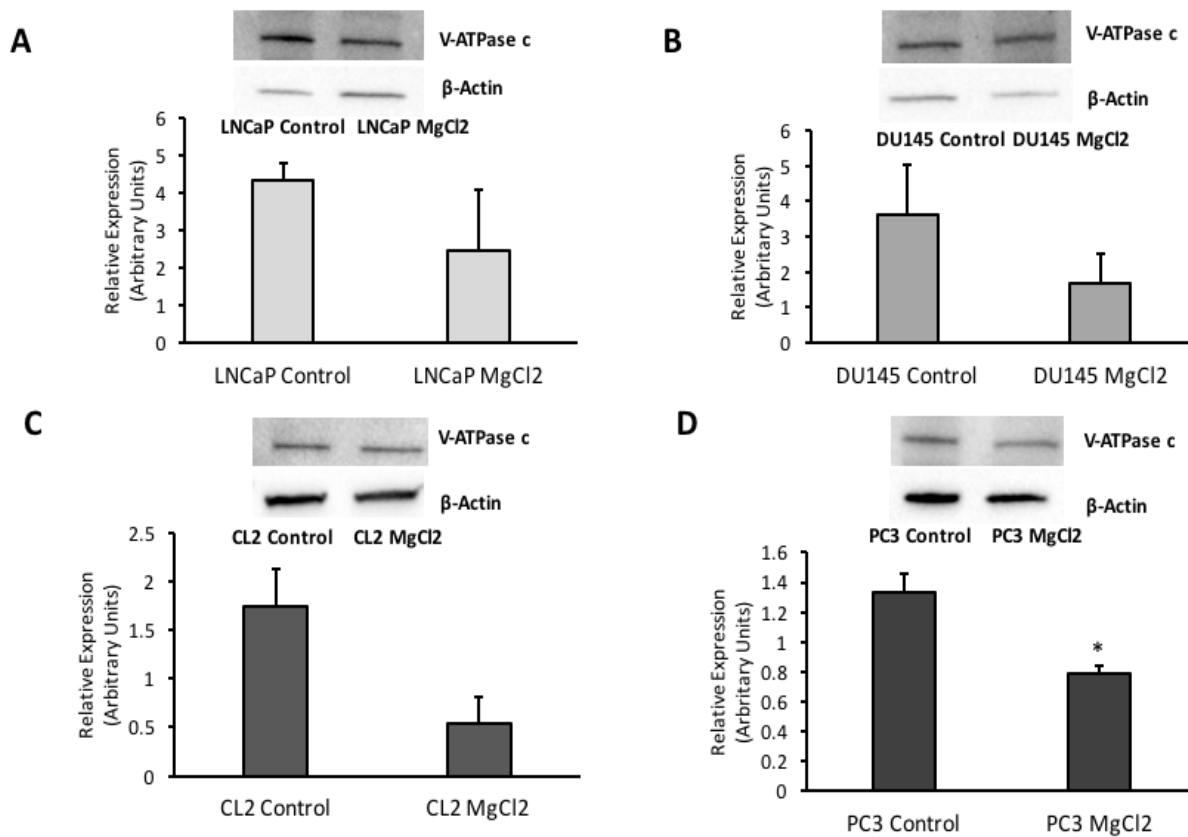


**Figure 3.** MgCl<sub>2</sub> decreases the expression of V-H<sup>+</sup>-ATPase. V-H<sup>+</sup>-ATPase c subunit expression and quantification in prostate cancer cells: LNCaP (A), DU145 (B), CL2 (C), and PC3 (D), both control and after 48 hours of MgCl<sub>2</sub> treatment (500  $\mu$ M); n=3. One-way ANOVA, \*p=0.013.

**MgCl<sub>2</sub> increases F-actin and Myosin II (NMII)**

To understand the mechanism underlying the decrease in migration speed induced by MgCl<sub>2</sub> treatment in prostate cancer cells, we evaluated the expression of F-actin in both control and after MgCl<sub>2</sub> (500  $\mu$ M) for 48 hours. Figure 4 shows F-actin staining in LNCaP (Figs.4A, B), DU145 (Figs. 4C, D), CL2 (Figs.4E, F), and PC3 (Figs.4G, H). MgCl<sub>2</sub> significantly increases F-actin, which explains the decrease in migration speed, and also increases cell stiffness [26]. This increase in F-actin and cell stiffness promises a potential new therapeutic role of MgCl<sub>2</sub> for decreasing cell motility and suppressing metastasis. Figure 5 shows the fluorescence intensity of F-actin in prostate cancer cells control and after treatment with MgCl<sub>2</sub> (500  $\mu$ M) for 48 hours. All prostate cancer cells LNCaP, DU145, CL2, and PC3 (Fig. 5) show significant increases in cortical F-actin induced by MgCl<sub>2</sub> treatment. NMII has a fundamental role in processes that require cellular reshaping and movement, such as cell adhesion, cell migration, and cell division [27, 28]. With these in mind, we evaluated the effect of MgCl<sub>2</sub> on NMII expression after 48 hours of treatment. Figure 6 shows the expression of NMII in prostate cancer cells control and after 48 hours of treatment with MgCl<sub>2</sub> (500  $\mu$ M), LNCaP (6A), DU145 (6B), CL2 (6C), and PC3 (6D). DU145 after MgCl<sub>2</sub> treatment resulted in a significant decrease in NMII expression compared to control. However, LNCaP, CL2, and PC3 did not show significant decreases in NMII expression due to the differential expression after the MgCl<sub>2</sub> treatment. The levels of expression of NMII in CL2 were very low compared to all the other cells. CL2 is a LNCaP parental but without androgen receptors. These variations could lead to differential expressions of proteins in general.

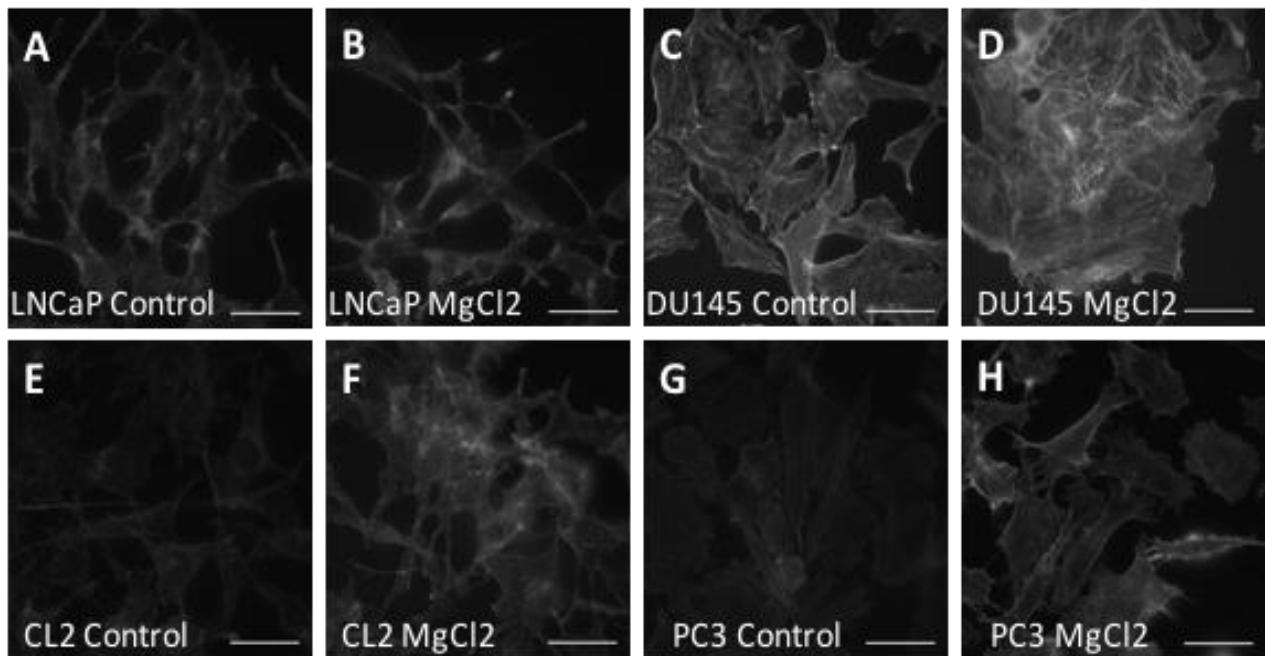


**Figure 4.** MgCl<sub>2</sub> significantly increases the expression of cortical F-actin. F-actin fluorescence stain by phalloidin alexa fluor 488 in prostate cancer cells: control and after 48 hours of MgCl<sub>2</sub> treatment (500 μM). LNCaP control (A) and treated (B); DU145 control (C) and treated (D); CL2 control (E) and treated (F); and PC3 control (G) and treated (H); n=3, scale bar = 33 μM.

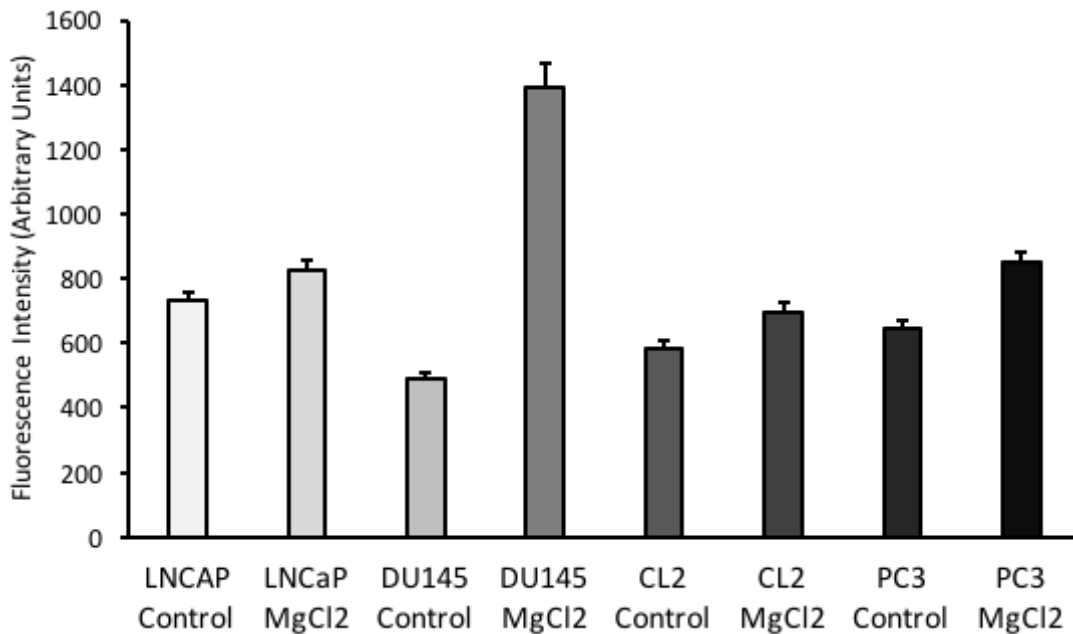


**Figure 5.** Increase of cortical F-actin induced by MgCl<sub>2</sub>. Fluorescence intensity of F-actin: control and after 48 hours of MgCl<sub>2</sub> treatment (500 μM); n=85 cells analyzed. One way ANOVA, comparison between LNCaP control vs. MgCl<sub>2</sub> p=0.009, DU145 control vs. MgCl<sub>2</sub> p<0.001, CL2 control vs. MgCl<sub>2</sub> p=0.0017, and PC3 control vs. MgCl<sub>2</sub> p<0.001.

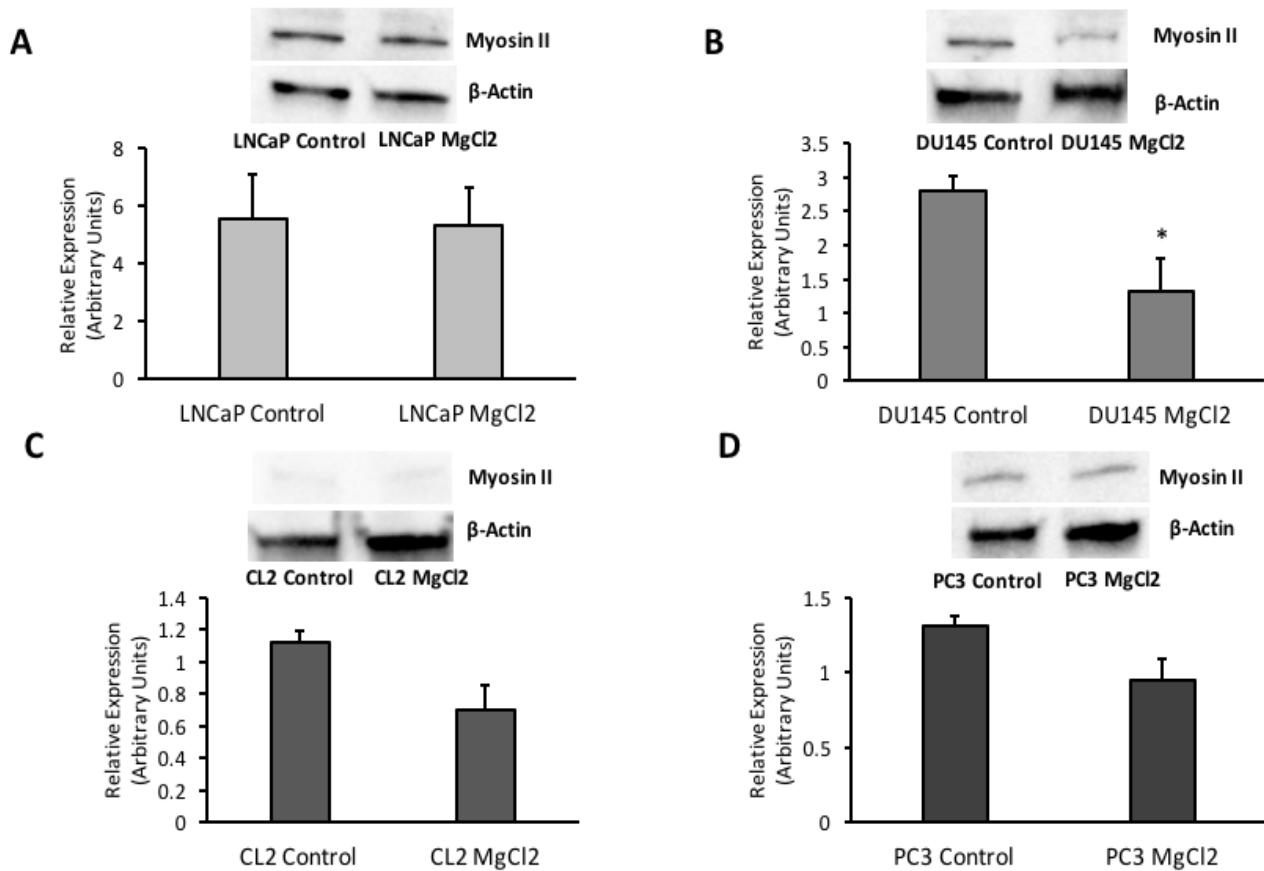


**Figure 6.** MgCl<sub>2</sub> decreases the expression of NMII in prostate cancer cells. NMIIB expression and quantification in LNCaP (A), DU145 (B), CL2 (C), and PC3 (D), both control and after 48 hours of MgCl<sub>2</sub> treatment (500  $\mu$ M); n=3. One way ANOVA, \*p=0.05.

***MgCl<sub>2</sub> Reverses the EMT by Decreasing Expression of Vimentin and Increasing Expression of E-cadherin***

To address the mechanism of action of MgCl<sub>2</sub> we evaluated the expression of the EMT marker vimentin in prostate cancer cells LNCaP (Fig.7A), DU145 (Fig.7B), CL2 (Fig.7C), and PC3 (Fig.7D), in the control and after 48 hours of MgCl<sub>2</sub> treatment (500  $\mu$ M). DU145 (Fig. 7B), with CL2 (Fig. 7C) demonstrating a significant decrease in vimentin expression after MgCl<sub>2</sub> treatment, showing a reversal of EMT caused by MgCl<sub>2</sub>. We also evaluated the expression of another EMT marker, namely E-cadherin. E-cadherin is a common feature of epithelial cells, and in order to acquire a mesenchymal phenotype during EMT most tumor cells lose or decrease this protein expression [29]. MgCl<sub>2</sub> (500  $\mu$ M) significantly increased the expression of E-cadherin for LNCaP (Fig. 8A), CL2 (Fig. 8C), and PC3 (Fig. 8D) but not for DU145 (Fig. 8B), which showed only an insignificant increase. These results revealed the role of MgCl<sub>2</sub> in EMT reversal in almost all cells evaluated. The E-cadherin expression difference observed may be due to the different tissue origins of these cells and presence or not of androgen receptors.

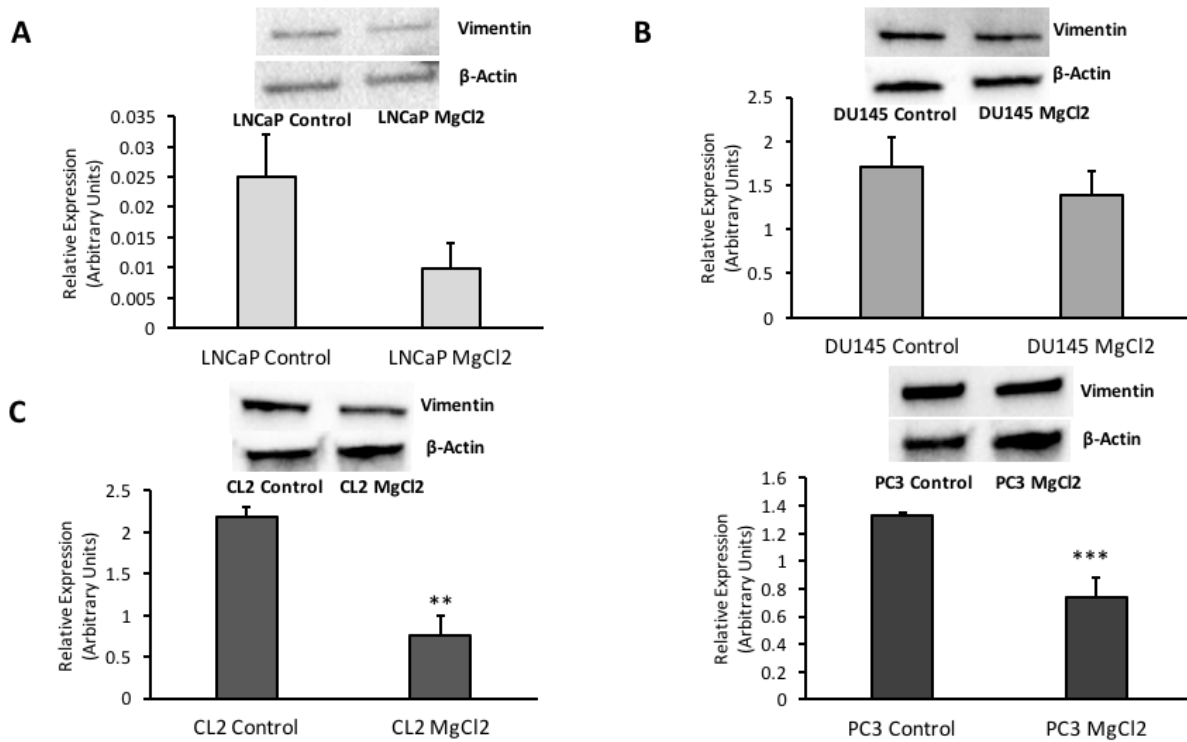


**Figure 7.** MgCl<sub>2</sub> decreases the expression of vimentin in prostate cancer cells, suggesting EMT reversal. Vimentin expression and quantification in LNCaP (A), DU145 (B), CL2 (C), and PC3 (D), both control and after 48 hours of MgCl<sub>2</sub> treatment (500  $\mu$ M); n=3. One way ANOVA, \*\*p=0.032, \*\*\*p=0.013.

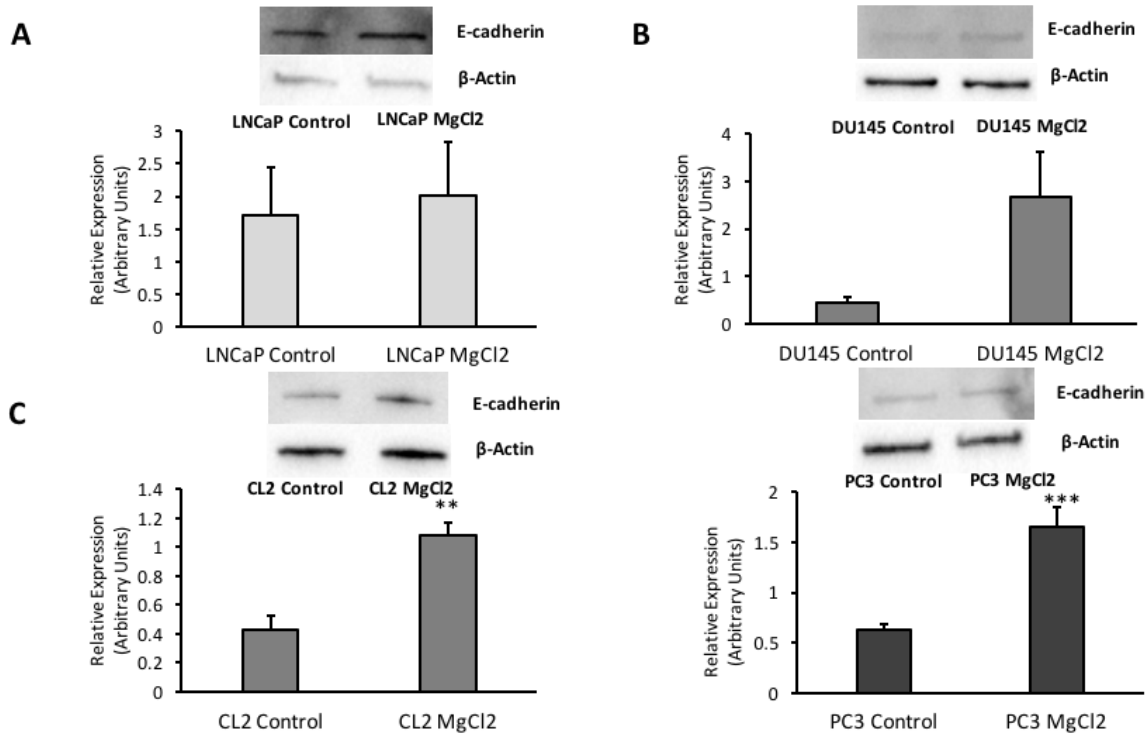


**Figure 8.** MgCl<sub>2</sub> increases the expression of E-cadherin in prostate cancer cells suggesting EMT reversal. E-cadherin expression and quantification in LNCaP (A), DU145 (B), CL2 (C), and PC3 (D) - both control and after 48 hours of MgCl<sub>2</sub> treatment (500  $\mu$ M); n=3. One way ANOVA, \*\*p=0.006, \*\*\*p=0.008.

### MgCl<sub>2</sub> Induces Chromatin Condensation and Decreases Transcription.

We also evaluated the nuclear changes induced by MgCl<sub>2</sub>, in the control, and after 48 hours of MgCl<sub>2</sub> treatment (500 μM). Figure 9 shows the nucleus staining in LNCaP (Figs. 9A, B); DU145 (Figs. 9C, D); CL2 (Figs. 9E, F), and PC3 (Figs. 9G, H). The nucleus fluorescence stain increased significantly after the MgCl<sub>2</sub> treatment, reflecting a chromatin condensation effect of MgCl<sub>2</sub> [30]. Figure 10 shows the fluorescence intensity of nuclear stain DAPI in prostate cancer cells control and after MgCl<sub>2</sub> treatment. All prostate cancer cells LNCaP, DU145, CL2, and PC3 (Fig. 10) show a significant increase in nuclear brightness that indicates chromatin condensation induced by MgCl<sub>2</sub> treatment. In some cells, presence of bright spots are evident after treatment, indicating chromatin condensation (Fig. 10). After revealing that MgCl<sub>2</sub> induces chromatin condensation we also evaluated the expression of the transcription factor NFκB in prostate cancer cells during both the control and after MgCl<sub>2</sub> treatment to corroborate this result. Figure 11 shows the expression of NFκB in prostate cancer cells LNCaP (11A), DU145 (11B), CL2 (11C), and PC3 (11D) control and after MgCl<sub>2</sub> treatment for 48 hours (500 μM).

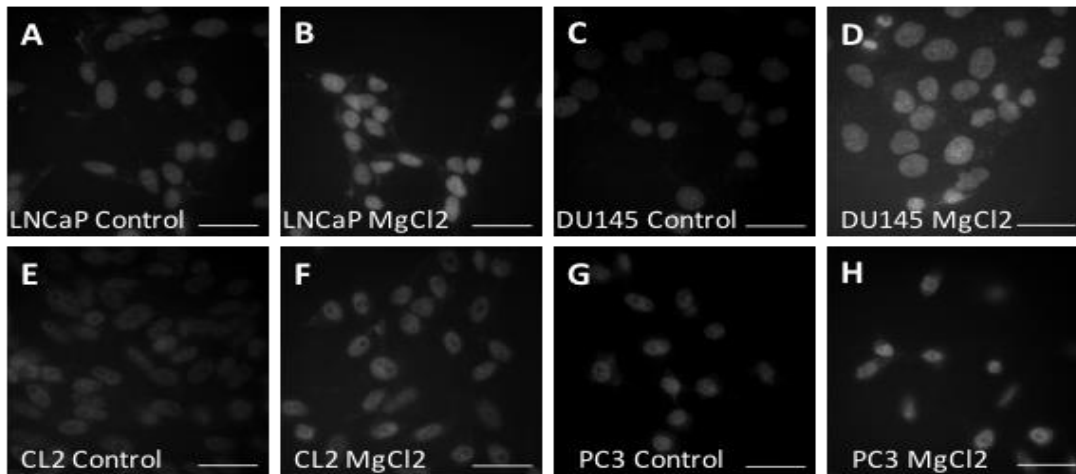


**Figure 9.** MgCl<sub>2</sub> increases chromatin condensation. Nuclear staining by DAPI in LNCaP (A and B), DU145 (C and D), CL2 (E and F), and PC3 (G and H), both control and after 48 hours of MgCl<sub>2</sub> treatment (500 μM); n=3, scale bar = 33 μM.

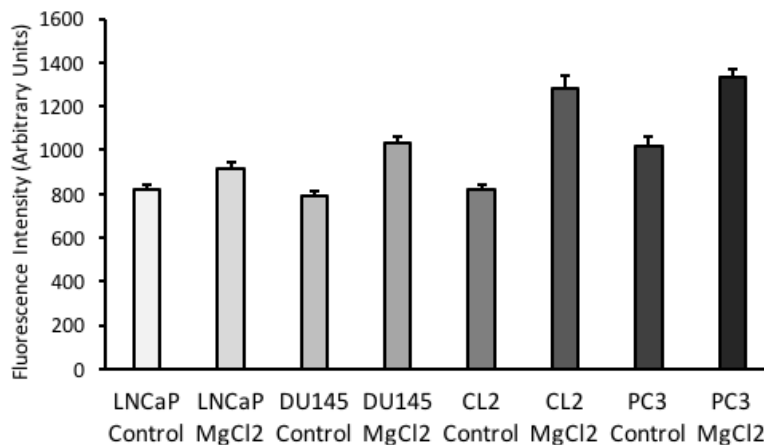


**Figure 10.** Increases in chromatin condensation induced by MgCl<sub>2</sub>. Fluorescence intensity of nucleus (DAPI): control and after 48 hours of MgCl<sub>2</sub> treatment (500 μM); n=85 cells analyzed. One way ANOVA, comparison LNCaP control vs. MgCl<sub>2</sub> p=0.016, DU145 control vs. MgCl<sub>2</sub> p<0.001, CL2 control vs. MgCl<sub>2</sub> p<0.001, and PC3 control vs. MgCl<sub>2</sub> p<0.001.

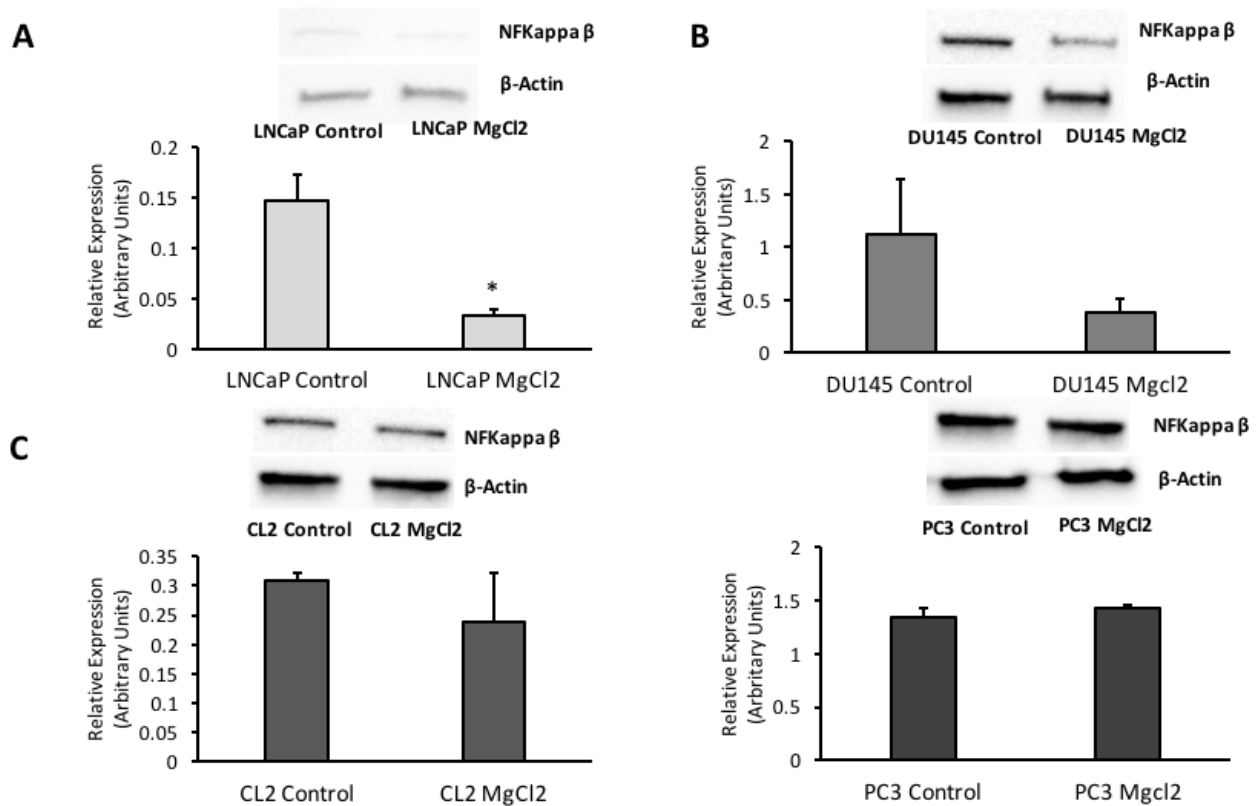


**Figure 11.** MgCl<sub>2</sub> decreases the expression of transcription factor NFκB in prostate cancer cells. NFκB expression and quantification in LNCaP (A), DU145 (B), CL2 (C), and PC3 (D), both during control and after 48 hours of MgCl<sub>2</sub> treatment (500 μM); n=3. One way ANOVA, \*p=0.012.

**DISCUSSION**

We believe we are the first study to show the beneficial effects of MgCl<sub>2</sub> (500 μM) on cell migration, V-H<sup>+</sup>-ATPase expression, and reversal of the EMT in prostate cancer. We find that MgCl<sub>2</sub> induces apoptosis of prostate cancer cells with androgen receptors (LNCaP) and without (CL2, DU145, and PC3). These results corroborate prior results showing induction of apoptosis by MgCl<sub>2</sub> in DU145 [2].

Following the cell viability degradation by MgCl<sub>2</sub>, we addressed the possible effects of MgCl<sub>2</sub> on cell migration by measuring the migration speed of cells, both without and with treatment. We varied the concentration following a prior study [2] and selected the concentrations: 25, 50, 200, 500 μM, and 1 mM. However, 500 μM produced the maximal decrease (about 30%) in migration speed. Thus, MgCl<sub>2</sub> is not only able to induce apoptosis but also to decrease cell motility. Our data, showing a remarkable decrease in cell migration speed, encourage further studies, involving other cancer types and in vivo models, to fully establish MgCl<sub>2</sub>'s role in suppressing metastasis.

V-H<sup>+</sup>-ATPase activation at the plasma membrane of tumor cells is known as a molecular marker for metastasis in human melanoma, pancreatic carcinoma, and breast cancer [9, 25, 31]. This pump is responsible for maintenance of pH that favors invasion and metastasis [9]. The extracellular acidification, caused by V-H<sup>+</sup>-ATPase extruding protons, activates secretion of proteases which facilitate degradation of the extracellular matrix and basement membrane and

alters cytoskeleton structure. However, the role of cell mechanical properties during invasion remains unclear [32]. For the first time, we show that  $MgCl_2$  decreases V-H<sup>+</sup>-ATPase expression in prostate cancer cells with different metastatic potentials. V-H<sup>+</sup>-ATPase c subunit expression is significantly reduced (by 30%) after  $MgCl_2$  treatment. This result reinforces the potential therapeutic role of  $MgCl_2$  targeting this pump that promotes invasion and metastasis.

A previous study demonstrated how an anticancer agent caused changes in morphology and F-actin distribution in leukemia cells [33]. This study is corroborated by our results showing that  $MgCl_2$  induces significant changes in cortical F-actin in all prostate cancer cells. The fluorescence intensity of F-actin is shown to increase by  $MgCl_2$  treatment. This F-actin increase suggests higher cell stiffness, which may explain the decrease in cell migration and resulting metastasis. It is known that cells sense the stiffness and spatial patterning of the microenvironment to modulate their own shape and cortical stiffness. However, the way substrate stiffness, cell shape, and cell stiffness affect each other is still unknown. It is clear how cell size and substrate stiffness can combine either to enhance or antagonize each other as well as affect cell morphology and mechanics [26]. Due to its effects on F-actin bundling and contractility, NMII acts as a key integrator of the processes that drive cell migration and adhesion. NMII is also an important end point on which many signaling pathways converge mainly through Rho GTPases [27, 28]. To address the other potential mechanical effects of  $MgCl_2$ , we evaluated the expression of NMII in prostate cancer cells control and after treatment with  $MgCl_2$ . We discovered  $MgCl_2$  decreased significantly the expression of NMII in DU145.

Other studies demonstrated how epithelial mesenchymal transition (EMT) plays a critical role in malignant transformation and in cancer progression, in addition to providing invasive and metastatic properties to cancer cells. EMT is important in embryo development during which epithelial cells acquire mesenchymal and fibroblast-like phenotypes and show reduced intercellular adhesion and increased motility. Several oncogenic pathways such as peptide growth factors, Src, Ras, Wnt/ $\beta$ -catenin, and Notch induce EMT. A critical molecular event in this transition is the down-regulation of the cell adhesion molecule: E-cadherin [29].  $MgCl_2$  plays a crucial role in the EMT reversal in prostate cancer cells. The reversal occurs by decreasing the expression of the mesenchymal marker vimentin and by increasing the expression of the epithelial marker E-cadherin. We show how DU145 and CL2 significantly decreased the expression of vimentin while LNCaP, CL2, and PC3, while significantly increasing the expression of E-cadherin. These differences are possibly due to the differences in tissue origins that determine the physiological role of each cell line. Additionally, the sensitivity to androgen receptors could also cause these different trends observed. LNCaP is an androgen sensitive cell line; its derived CL2 clone is androgen receptor negative [34]. DU145, moderately metastatic and androgen receptor negative, was obtained from a brain metastasis [20]. PC3, also a highly metastatic cell line that does not express androgen receptors [21], was obtained from a bone metastasis [22].

We also find a significant increase in nuclear chromatin condensation with  $MgCl_2$  treatment in all prostate cancer cells. This result corroborates previous studies that demonstrated that anticancer agents can induce chromatin condensation. Additionally, other studies have shown how chromatin is negatively charged, and as a result how the condensed state of nuclei and their chromatin depend on the cation concentration in the environment. Thus, a low concentration of

cations such as  $Mg^{2+}$  leads to decondensation of chromatin and expansion of the nucleus, while the presence of  $Mg^{2+}$  leads to chromatin condensation [35]. Since increased chromatin condensation can reduce cell transcription, we evaluated the expression of the transcription factor NFkB which is usually over-expressed in many cancer types. A prior study demonstrated how blockade of NFkB affected angiogenesis, growth, and metastasis of prostate cancer in mouse model. Thus, the reduced angiogenesis by blocking NFkB is the result of the inhibition of three important proangiogenic molecules: interleukin 8 (IL8), vascular endothelial growth factor (VEGF), and metalloproteinase 9 (MMP-9). Inhibition of NFkB activity in PC-3M cells also down regulated MMP-9 mRNA and collagenase activity, resulting in decreased invasion through matrigel [36]. Our data demonstrates how  $MgCl_2$  decreased the expression of NFkB in prostate cancer cells, corroborating this previous study which revealed how inhibition of this transcription factor prevents cancer invasion, metastasis, and growth.

In summary, we evaluated the effect of  $MgCl_2$  in prostate cancer cells which are lowly metastatic and sensitive to androgen receptor (LNCaP), moderately metastatic insensitive to androgen receptor (DU145), and highly metastatic insensitive to androgen receptor (CL2 and PC3).  $MgCl_2$  induced morphological changes and apoptosis, reduced the migration speed, increased cortical F-actin, decreased NMII expression, increased chromatin condensation, decreased transcription factor NFkB expression, and caused EMT reversal (by reducing the expression of vimentin and by increasing the expressions of E-cadherin and F-actin). Future studies should explore the preventive and possible therapeutic role of  $MgCl_2$  using in vivo studies as well as extending to other cancer types.

## CONCLUSION

We evaluated the effect of  $MgCl_2$  in prostate cancer cells which are non-tumorigenic and sensitive to androgen receptor (LNCaP), moderately metastatic insensitive to androgen receptor (DU145), and highly metastatic insensitive to androgen receptor (CL2 and PC3).  $MgCl_2$  induced apoptosis, reduced the migration speed, increased cortical F-actin, decreased NMII expression, increased chromatin condensation, decreased transcription factor NFkB expression, and reversed EMT (by reducing the expression of vimentin and by increasing the expression of E-cadherin and F-actin). Future studies should explore the preventive and possible therapeutic roles of  $MgCl_2$  in vivo and extending to other cancer types.

**List of Abbreviations:**  $MgCl_2$ , magnesium chloride; EMT, epithelial mesenchymal transition; NMII, myosin II; NFkB, NF Kappa B;  $Mg^{2+}$ , magnesium; CRC, colorectal cancer; FBS, fetal bovine serum; PBS, Phosphate Buffer Saline; IL8, interleukin 8; VEGF, vascular endothelial growth factor; MMP-9, metalloproteinase 9.

**Competing Interests:** The authors have no financial interests or conflicts of interest.

**Authors' Contributions:** All authors contributed to this study.

**Acknowledgments and Funding:** We would like to thank Dr. Khan for reviewing our manuscript. This research did not receive any specific grant from funding agencies in the public, commercial, or not-for-profit sectors.

**REFERENCES**

1. Swaminathan R: Disorders of magnesium metabolism. *CPD Bulletin of Clinical Biochemistry* 2000, 2: 3–12.
2. Oseni SO, Quiroz E, Kumi-diaka J: Chemopreventive Effects of Magnesium Chloride Supplementation on Hormone Independent Prostate Cancer Cells. *Functional Foods in Health and Disease* 2016, 6: 1–15.
3. Patisroglu T, Sahin G, Kontas O, Uzum K, Saraymen R: Protective effect of magnesium supplementation on experimental 3-methyl cholanthrene-induced fibrosarcoma and changes in tissue magnesium distribution during carcinogenesis in rats. *Biological Trace Elements Research* 1997, 56: 179–185.
4. Guerrero M, Volpe S, Mao J: Therapeutic Uses of Magnesium. *American Family Physician* 2009, 80: 157–162.
5. Paolisso G, Scheen A, D’Onofrio F, Lefebvre P: Magnesium and glucose homeostasis. *Diabetologia* 1990, 33: 511–514.
6. Lajer H, Kristensen M, Hansen HH, Nielsen S, Frokiaer J, Ostergaard LF, et al.: Magnesium depletion enhances cisplatin-induced nephrotoxicity. *Cancer Chemotherapy Pharmacology* 2005, 56: 535–542.
7. Willox JC, McAllister EJ, Sangster G, Kaye SB: Effects of magnesium supplementation in testicular cancer patients receiving cis-platin: a randomised trial. *British Journal of Cancer* 1986, 54: 19–23.
8. Chen GC, Pang Z, Liu QF: Magnesium intake and risk of colorectal cancer: a meta-analysis of prospective studies. *European Journal of Clinical Nutrition*, 2012, 66: 1182–1186.
9. Sennoune SR, Bakunts K, Martínez GM, Chua-Tuan JL, Kebir Y, Attaya MN, et al.: Vacuolar H<sup>+</sup>-ATPase in human breast cancer cells with distinct metastatic potential: distribution and functional activity. *American Journal of Physiology Cell Physiology* 2004, 286: C1443–C1452.
10. Hinton A, Sennoune SR, Bond S, Fang M, Reuveni M, Sahagian GG, et al.: Function of a subunit isoforms of the V-ATPase in pH homeostasis and in vitro invasion of MDA-MB231 human breast cancer cells. *Journal of Biological Chemistry* 2009, 284: 16400–16408.
11. Lamouille S, Connolly E, Smyth JW, Akhurst RJ, Derynck R: TGF-beta-induced activation of mTOR complex 2 drives epithelial-mesenchymal transition and cell invasion. *Journal of Cell Science* 2012, 125: 1259–1273.
12. Sarrio D, Rodriguez-Pinilla SM, Hardisson D, Cano A, Moreno-Bueno G, Palacios J: Epithelial-mesenchymal transition in breast cancer relates to the basal-like phenotype. *Cancer Research* 2008, 68: 989–997.
13. Lamouille S, Xu J, Derynck R: Molecular mechanisms of epithelial-mesenchymal transition. *Nature Reviews Molecular Cell Biology* 2014, 15: 178–196.
14. Hollier BG, Evans K, Mani SA: The epithelial-to-mesenchymal transition and cancer stem cells: A coalition against cancer therapies. *Journal of Mammary Gland Biology*

- and Neoplasia 2009, 14: 29–43.
15. Mani SA, Guo W, Liao MJ, Eaton EN, Ayyanan A, Zhou AY, et al.: The Epithelial-Mesenchymal Transition Generates Cells with Properties of Stem Cells. *Cell* 2008, 133: 704–715.
  16. Kalluri R, Weinberg R: Review series The basics of epithelial-mesenchymal transition. *Journal of Clinical Investigation* 2009, 119: 1420–1428.
  17. Jemal A, Bray F, Ferlay J: Global Cancer Statistics. *CA Cancer Journal for Clinicians* 2011, 49: 33-64.
  18. Medeiros R, Vasconcelos A, Costa S, Pinto D, Lobo F, Morais A, et al.: Linkage of angiotensin I-converting enzyme gene insertion/deletion polymorphism to the progression of human prostate cancer. *The Journal of Pathology* 2004, 202: 330–335.
  19. Tso C, McBride WH, Sun J, Patel B, Tsui K, Paik SH, Gitlitz B, et al.: Androgen deprivation induces selective outgrowth of aggressive hormone-refractory prostate cancer clones expressing distinct cellular and molecular properties not present in parental androgen-dependent cancer cells. *Cancer Journal* 2000, 6: 220–233.
  20. Nishimura K, Kitamura M, Takada S, Nonomura N, Tsujimura, Matsumiya K, et al.: Regulation of invasive potential of human prostate cancer cell lines by hepatocyte growth factor. *International Journal of Urology* 1998, 5: 276–281.
  21. Tai S, Sun Y, Squires JM, Zhang H, Oh WK, Liang CZ, et al.: PC3 is a cell line characteristic of prostatic small cell carcinoma. *Prostate* 2011, 71: 1668–1679.
  22. Kaighn ME, Narayan KS, Ohnuki Y, Lechner JF, Jones LW: Establishment and characterization of a human prostatic carcinoma cell line (PC-3). *Investigative Urology* 1979, 17: 16–23.
  23. Valster A, Tran NL, Nakada M, Berens ME, Chan AY, Symons M: Cell migration and invasion assays. *Methods* 2005, 37: 208–215.
  24. Van Engeland M, Nieland LJW, Ramaekers FC, Reutelingsperger PMC: Annexin V-Affinity Assay: A Review on an Apoptosis Detection System Based on Phosphatidylserine Exposure. *Cytometry* 1998; 31:1–9.
  25. Cotter K, Capecci J, Sennoune S, Huss M, Maier M, Martinez-Zaguilan R, et al.: Activity of Plasma Membrane V-ATPases Is Critical for the Invasion of MDA-MB231 Breast Cancer Cells. *Journal of Biological Chemistry* 2015; 290: 3680–3692.
  26. Tee SY, Fu J, Chen CS, Janmey PA: Cell shape and substrate rigidity both regulate cell stiffness. *Biophysical Journal* 2011, 100: L25–L27.
  27. Vicente-Manzanares M, Ma X, Adelstein R, Horwitz A: Non-muscle myosin II takes centre stage in cell adhesion and migration. *Nature Reviews Molecular Cell Biology* 2009, 10: 778–790.
  28. Vicente-Manzanares M, Ma X, Adelstein RS, Horwitz AR: Non-muscle myosin II takes centre stage in cell adhesion and migration. *Nature Reviews Molecular Cell Biology* 2009, 10: 778–790.
  29. Larue L, Bellacosa A: Epithelial–mesenchymal transition in development and cancer: role of phosphatidylinositol 3 0 kinase/AKT pathways. *Oncogene* 2005: 7443–7454.

30. Rajadhyaksha M, Menaker G, Flotte T, Dwyer PJ, González S: Confocal examination of nonmelanoma cancers in thick skin excisions to potentially guide mohs micrographic surgery without frozen histopathology. *Journal of Investigative Dermatology* 2001, 117: 1137–1143.
31. Santos JM, Martinez-Zaguilan R, Facanha AR, Hussain F, Sennoune S: Vacuolar H-ATPase in the nuclear membranes regulates nucleo-cytosolic proton gradients. *American Journal of Physiology Cell Physiology* 2016, 311: C547–C558.
32. Swaminathan V, Mythreye K, Tim O'Brien E, Berchuck A, Blobe GC, Superfine R: Mechanical Stiffness grades metastatic potential in patient tumor cells and in cancer cell lines. *Cancer Research* 2011, 71: 5075–5080.
33. Grzanka A: Actin distribution patterns in HL-60 leukemia cells treated with etoposide. *Acta Histochemica* 2001, 103:453–464.
34. Horoszewicz JS, Leong SS, Kawinski E, Horoszewicz JS, Leong SS, Kawinski E, et al.: LNCaP Model of Human Prostatic Carcinoma LNCaP Model of Human Prostatic Carcinoma. *Cancer Research* 1983, 43: 1809–1818.
35. Imai R, Komeda S, Shimura M, Tamura S, Nishimura K, Rogge R, et al.: Chromatin folding and DNA replication inhibition mediated by a highly antitumor-active tetrazolato-bridged dinuclear platinum(II) complex. *Nature Publication Group* 2016, 6: 1–34.
36. Huang S, Pettaway CA, Uehara H, Bucana CD FI: Blockade of NF-kB activity in human prostate cancer cells is associated with suppression of angiogenesis, invasion, and metastasis. *Oncogene* 2001, 20: 4188– 4197.